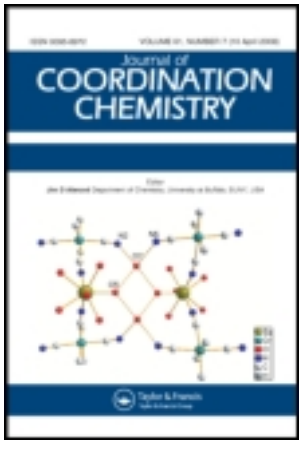

Journal of Coordination Chemistry
Publication details, including instructions for authors and subscription information:
http://www.tandfonline.com/loi/gcoo20

Cation-templated 2-D Mn(II)-oxalate framework with an acyclic tetrameric water cluster

Kafeel Ahmad Siddiqui [a b], Gopal K. Mehrotra [a] & Jerzy Mrozinski [c]

[a] Department of Chemistry, Motilal Nehru National Institute of Technology, Allahabad-211004, U.P., India

[b] Solid State and Structural Chemistry Unit, Indian Institute of Science, Bangalore-560012, India

[c] Faculty of Chemistry, Wroclaw University, F. Joliot-Curie 14 Street, 50-383 Wroclaw, Poland

Published online: 12 Jul 2011.

To cite this article: Kafeel Ahmad Siddiqui, Gopal K. Mehrotra & Jerzy Mrozinski (2011) Cation-templated 2-D Mn(II)-oxalate framework with an acyclic tetrameric water cluster, Journal of Coordination Chemistry, 64:13, 2367-2376, DOI: 10.1080/00958972.2011.586031

To link to this article: http://dx.doi.org/10.1080/00958972.2011.586031

Journal of Coordination Chemistry
Vol. 64, No. 13, 10 July 2011, 2367–2376

Cation-templated 2-D Mn(II)–oxalate framework with an acyclic tetrameric water cluster

KAFEEL AHMAD SIDDIQUI*†‡, GOPAL K. MEHROTRA† and JERZY MROZINSKI§

†Department of Chemistry, Motilal Nehru National Institute of Technology, Allahabad-211004, U.P., India
‡Solid State and Structural Chemistry Unit, Indian Institute of Science, Bangalore-560012, India
§Faculty of Chemistry, Wroclaw University, F. Joliot-Curie 14 Street, 50-383 Wroclaw, Poland

(*Received 9 December 2010; in final form 16 April 2011*)

The single-crystal X-ray structure of a cation-templated manganese–oxalate coordination polymer $[NH(C_2H_5)_3][Mn_2(ox)_3]\cdot(5H_2O)]$ (**1**) is reported. In **1**, triethylammonium cation is entrapped between the cavities of 2-D honeycomb layers constructed by oxalate and water. The acyclic tetrameric water clusters and discrete water assemble the parallel 2-D honeycomb oxalate layers *via* an intricate array of hydrogen bonds into an overall 3-D network. The magnetic susceptibility, with and without the water cluster, are reported with infrared and EPR studies.

Keywords: Mn–oxalate framework; Encapsulated triethylammonium cation; Tetrameric water cluster

1. Introduction

The supramolecular association of water forming discrete clusters in the voids of coordination polymers continues to attract a great deal of attention due to the fundamental importance of water in many physical, chemical, and biological processes [1, 2]. Hydrogen-bonding interactions between water aggregates and the surroundings often play a key role in stabilizing water clusters with diverse morphologies within the crystal lattices of the metal–organic frameworks (MOFs) [3–7]. Here both water–MOF and water–water interactions can be important in lending stability to the overall structure [8–18]. The water tetramer, present as a principal species in liquid water, has drawn attention as many important physical properties such as heat capacity of liquid water have been studied through them [19, 20]. Among the various theoretically possible configurations, the water tetramer commonly adopts a cyclic planar or a quasi planar structure with all four water molecules acting as both proton donors and

*Corresponding author. Email: ahmad_kafeel@rediffmail.com

ISSN 0095-8972 print/ISSN 1029-0389 online © 2011 Taylor & Francis
DOI: 10.1080/00958972.2011.586031

acceptors [21–24]. An acyclic water tetramer, a high-energy species, is relatively rare and has been identified in the constrained environments of the cavities of MOFs [25–28]. A major challenge in molecular magnetism is the synthesis of multifunctional magnets and in this context, oxalate-based bimetallic networks of general formula A $[M_1M_2^{III}(ox)_3]$ (with $M_1 = Li^+$, Na^+, Mn^{2+}, ...; $M_2^{III} = Cr$, Co, Fe, Ru; $ox = (C_2O_4)_{2-}$ and A^{n+} a counter cation) are widely studied compounds. These oxalate-based materials are composed of 2-D honeycomb anionic layers with counter cations between the layers. Some of these cations and other chemical building blocks can introduce a new physical function in the material such as non-linear optics; (supra) conduction or chirality as a result of asymmetric formation of these networks [29].

We report herein the synthesis and characterization of $[NH(C_2H_5)_3][Mn_2(ox)_3]\cdot(5H_2O)]$ (**1**) and the identification of acyclic tetramers in its crystal lattice. The single-crystal X-ray structure of **1** is presented and discussed. Infrared (IR), magnetic susceptibility, and EPR studies of the synthesized compound are also presented; magnetic susceptibility of **1**, with and without the water cluster, is discussed.

2. Experimental

All chemicals of reagent grade were commercially available and used without purification. Microanalysis data for the compound were obtained from CDRI, Lucknow. IR spectra were recorded on a Perkin-Elmer Model 1320 FTIR spectrometer as KBr pellets from 4000 to 500 cm^{-1}. X-ray powder diffraction was performed with a Bruker CCD area detector diffractometer, equipped with a graphite monochromator and Mo-Kα radiation ($\lambda = 0.71073$ Å). Magnetization measurements of polycrystalline samples were carried out with a Quantum Design SQUID magnetometer (MPMSXL-5-type) at a magnetic field of 0.5 T from 1.8–300 K. EPR spectra were recorded on a Bruker ESP 300 spectrometer operating at X-band equipped with an ER 035 M Bruker NMR gaussometer and HP 5350B Hewlett-Packard microwave frequency counter.

2.1. *Synthesis*

Solvothermal reaction between $[Mn(CH_3COO)_2]\cdot 4H_2O$ (147 mg), oxalic acid (75 mg), and triethylamine (0.25 mL) in a solvent mixture of DMF (2 mL) and DI water (2 mL) was carried out in an autogenous pressure Teflon-lined steel reactor at 180°C for 3 days. The homogeneous colorless solution obtained after slow cooling was filtered and the filtrate left undisturbed at room temperature for evaporation. After 45 days colorless crystals of $[NH(C_2H_5)_3][Mn_2(ox)_3]\cdot(5H_2O)]$ (**1**) were collected (49% yield). Elemental analysis: Calcd (%): C, 23.00; H, 4.15; N, 2.23. Found (%): C, 22.78; H, 4.12; N, 2.23.

2.2. *Crystallography*

A single crystal of $[NH(C_2H_5)_3][Mn_2(ox)_3]\cdot(5H_2O)]$ (**1**) with dimensions 0.13 mm × 0.10 mm × 0.08 mm was mounted on a CCD area detector diffractometer equipped with a graphite monochromator and Mo-Kα radiation ($\lambda = 0.71073$ Å). The unit cell dimensions and intensity data were measured at 293(2) K. The structure was solved by

Table 1. Crystal data and structure refinement of **1**.

Empirical formula	$C_{12}H_{26}Mn_2NO_{17}$
Formula weight ($g\,mol^{-1}$)	626.37
Temperature (K)	293(2)
Wavelength	0.71069
Crystal system	Monoclinic
Space group	*P 1 21/n 1 (14)*
Unit cell dimensions (Å, °)	
a	9.963(5)
b	16.679(5)
c	15.140(5)
α	90.000(5)
β	94.1619(5)
γ	90.000(5)
Volume ($Å^3$), *Z*	2509.23(192), 4
Calculated density ($g\,cm^{-3}$)	1.65796
Absorption coefficient (mm^{-1})	1.064
F(000)	1280
Crystal size (mm^3)	$0.13 \times 0.10 \times 0.08$
θ range for data collection	2.37–28.41
Limiting indices	$-13 \le h \le 13$; $-22 \le k \le 16$; $-18 \le l \le 20$
Reflections collected	16,022
Independent reflections	6168 [R(int) = 0.0854]
Completeness to θ	25.00°
Max. and min. transmission	0.9197 and 0.8740
Refinement method	Full-matrix least-squares on F^2
Data/restraints/parameters	6168/0/293
Goodness-of-fit on F^2	1.047
Final R indices [$I > 2\sigma(I)$]	$R_1 = 0.1776$; $wR_2 = 0.3608$
R indices (all data)	$R_1 = 0.1032$; $wR_2 = 0.2818$
Largest difference peak and hole ($e\,Å^{-3}$)	2.032 and −0.917

direct methods and refined by full-matrix least-squares based on F^2 with anisotropic thermal parameters for the non-hydrogen atoms using Bruker, SMART (data collection and cell refinement), Bruker SAINT (data reduction), SHELX-97 (structure solution), SHELXL-97 (structure refinement), and Bruker SHELXTL (molecular graphics) [30–33]. A multi-scan adsorption correction (SADABS) was applied. The waters are disordered and could not be solved.

2.3. *Crystal data for 1*

Crystal refinement data are listed in table 1. CCDC reference number 687270. These data can be obtained free of charge from The Cambridge Crystallographic Data Centre *via* www.ccdc.ac.uk/data_request/cif.

3. Results and discussion

3.1. *Description of the structure of 1*

The single-crystal X-ray diffraction studies reveal that **1** consists of anionic $[Mn_2(Ox)_3]^-$ framework with triethylammonium ensuring electroneutrality of the compound.

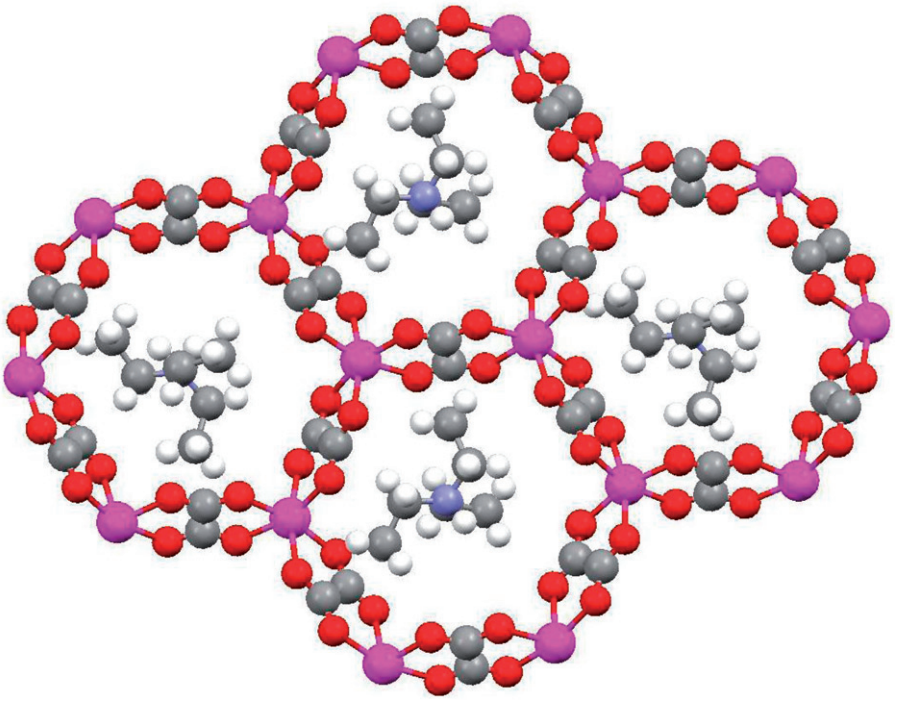

Figure 1. View of the crystal lattice showing encapsulated triethylammonium cation within the 2-D honeycomb layers along the *c*-axis.

Each asymmetric unit contains two crystallographically independent Mn^{2+} with similar coordination environments. Each Mn^{2+} has six-coordinate octahedral geometry with six oxygens from three different oxalates. The remaining oxygens from each oxalate extend the network into a hexagonal 2-D honeycomb structure. The triethylammonium template layer is ordered in the channel system (dimension $11.030 \times 11.697\,Å^2$) along the *c*-axis (figure 1). A closer examination of the crystal packing reveals the presence of two types of water, discrete water, and acyclic water tetramers, constituting a H-bonded extra-framework layer. The acyclic tetrameric water clusters and discrete water molecule self-assemble the 2-D honeycomb oxalate layers *via* an intricate array of hydrogen bonds into a 3-D network (figure 2).

The triethylammoniums trapped in the crystal lattice are also involved in H-bonding interactions with water (N1 $\cdots$ O1W 2.76 Å). This is indicative of its role as a structure directing template in addition to charge neutrality in **1**.

3.2. *IR spectra*

The IR spectrum (Supplementary material, figure S1a) of the complex shows a broad band centered around $3422\,cm^{-1}$ which vanishes on heating the compound under vacuum (0.1 mm) at 120°C for 2 h due to the escape of water from the lattice (Supplementary material, figure S1b). A deliberate exposure to water vapor for 2 days

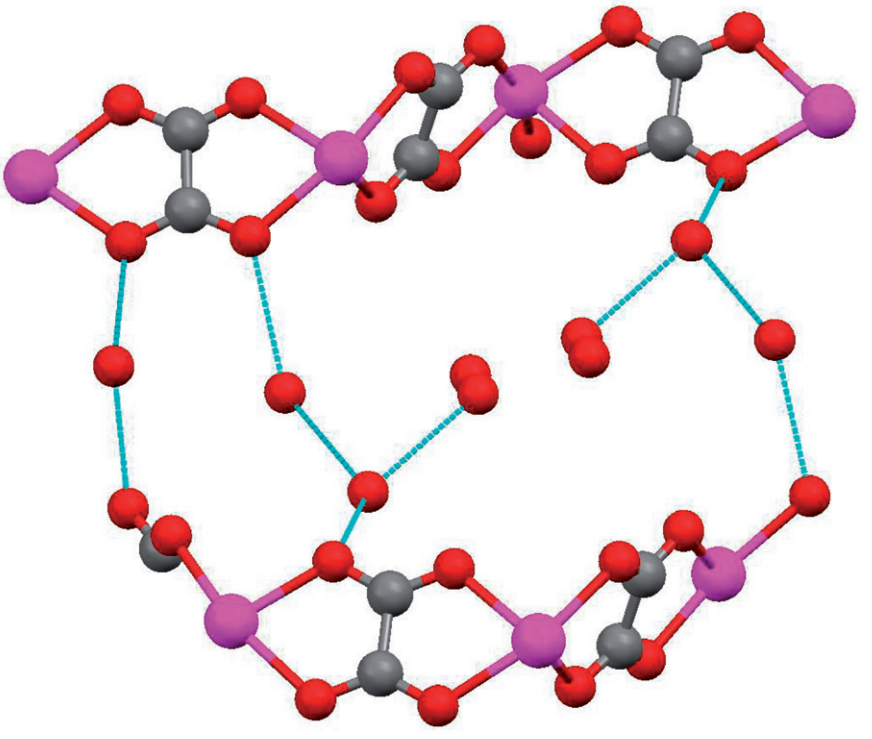

Figure 2. View of the 3-D framework formed by hydrogen bonding of the lattice water in **1**.

does not lead to re-absorption of water into the lattice as monitored by FTIR spectroscopy. The O–H stretching vibration of small water clusters $(H_2O)_n$ ($n = 2$–10) in the gaseous state have been investigated using IR spectroscopy, and this vibration has been found to be size specific over a wide range from 3720 to 2935 cm^{-1}. In comparison, the O–H stretching vibration in ice appears at 3220 cm^{-1}, while in liquid it shifts from 3280 to 3490 cm^{-1}. Therefore, the O–H stretching vibration of the water cluster in **1** is closer to liquid water with a slight variation attributed to its surroundings.

3.3. *Magnetic and EPR properties*

The magnetic properties of **1** were determined from 1.8 to 300 K in 0.5 T. The plots of magnetic susceptibility χ_M and the $\chi_M T$ product *versus* T are given in figure 3(a). The value of $\chi_M T$ is 7.30 $cm^3\,mol^{-1}\,K$ (7.66 B.M.) per two Mn^{2+} at room temperature, which is lower than that expected for uncoupled manganese(II) ion ($g = 2.0$, 4.38 $cm^3\,mol^{-1}\,K$). As the temperature decreases, the value of $\chi_M T$ decreases continuously upon cooling. In the low-temperature range (below 50 K) more evident decrease in its value is observed with continuous decrease of temperature, reaching 0.524 $cm^3\,mol^{-1}\,K$ (2.05 B.M.) at 1.8 K, indicating the occurrence of an antiferromagnetic interaction between manganese ions. It can be assumed that the hydrogen-bonded

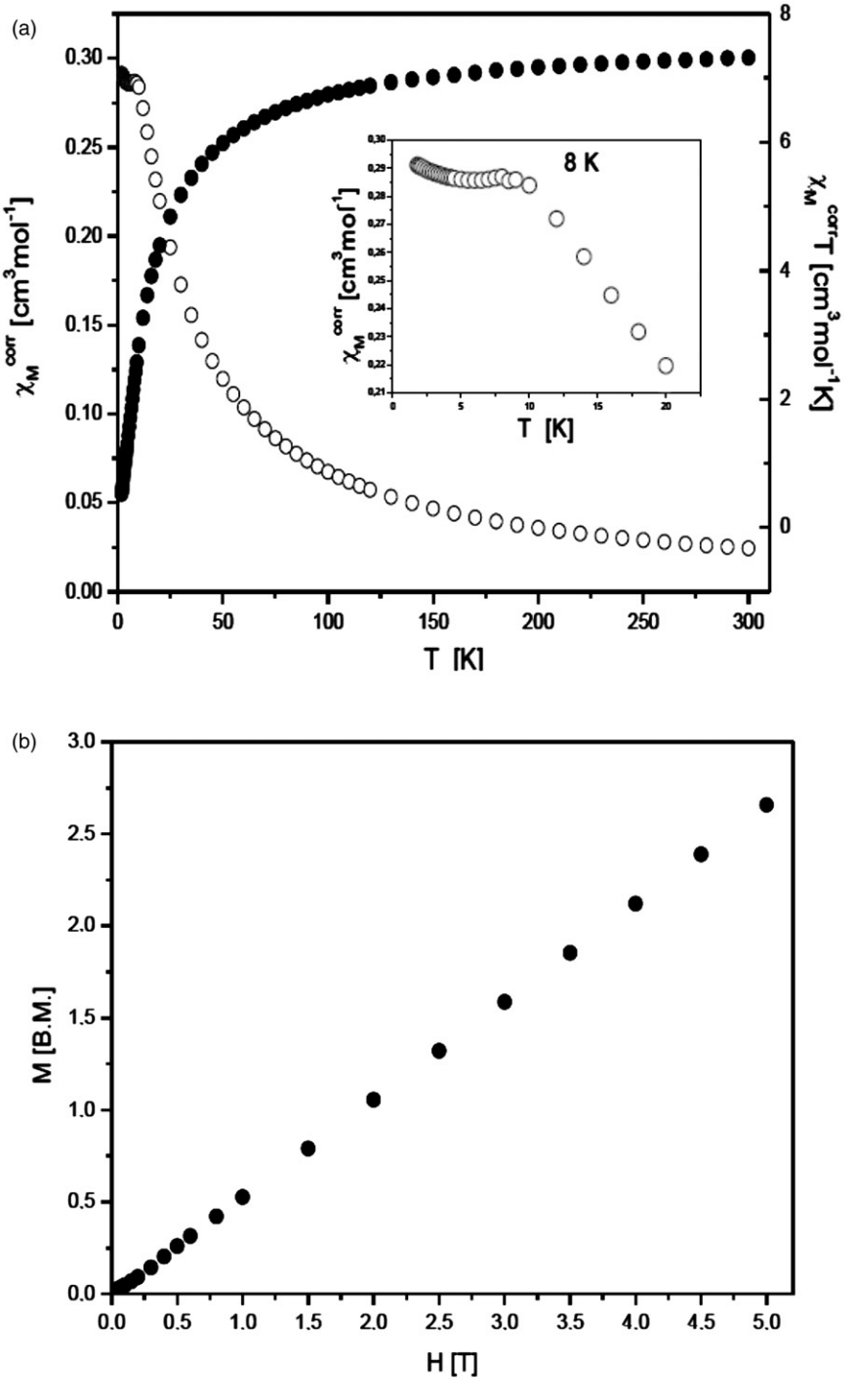

Figure 3. (a) Plot of χ_M (o) and $\chi_M T$ (•) *vs.* T for **1**. The solid line is the result of the best fit obtained with the parameters reported in the text. (b) Field dependence of the magnetization for **1** at 2 K (•).

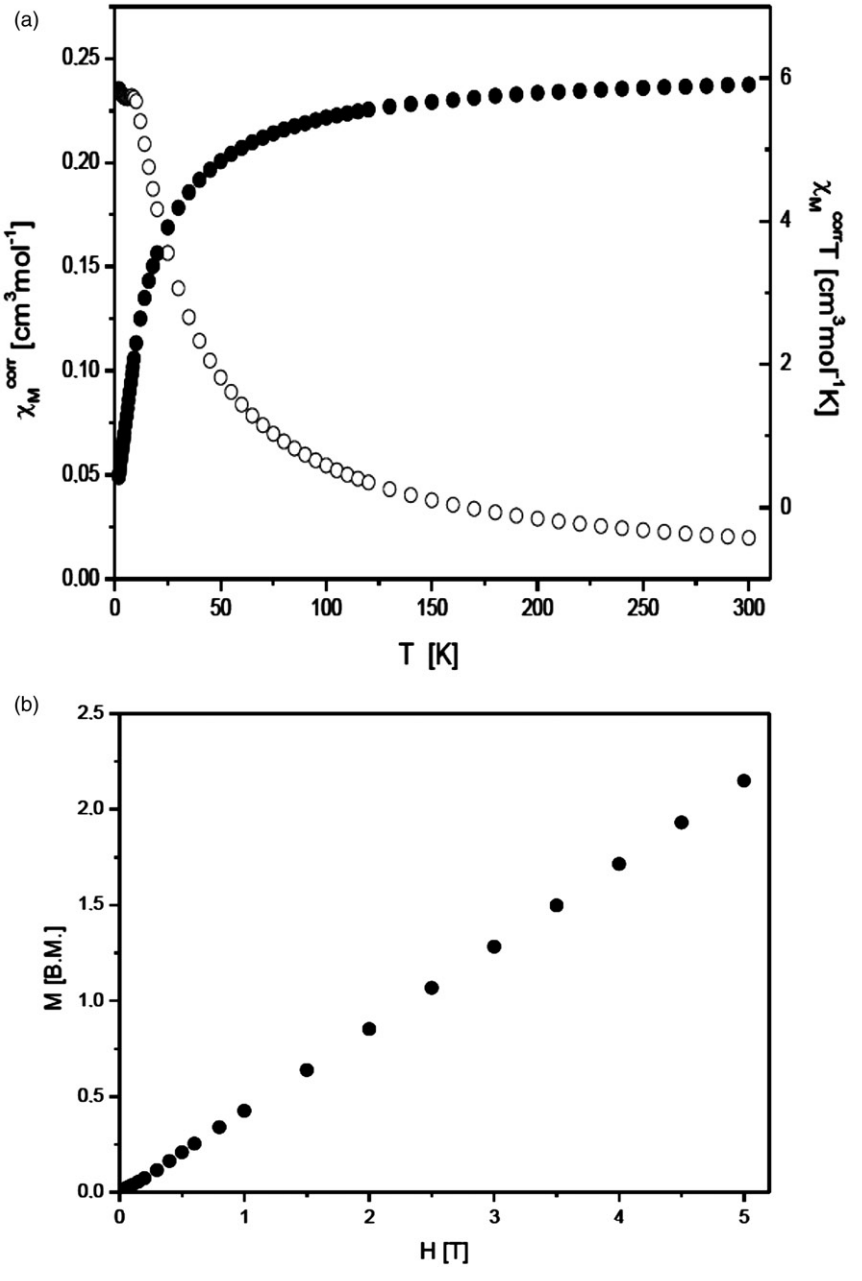

Figure 4. (a) Plot of χ_M (o) and $\chi_M T$ (•) *vs.* T for **1** without water. The solid line is the result of the best fit obtained with the parameters reported in the text. (b) Field dependence of the magnetization for dehydrated **1** at 2 K (•).

water groups provide important exchange pathways between Mn^{2+} centres (figure 3), probably by spin polarization mechanism [18]. The susceptibility curve exhibits a maximum, indicating the presence of antiferromagnetic ordering with a Néel temperature (T_N) of 8.00 K.

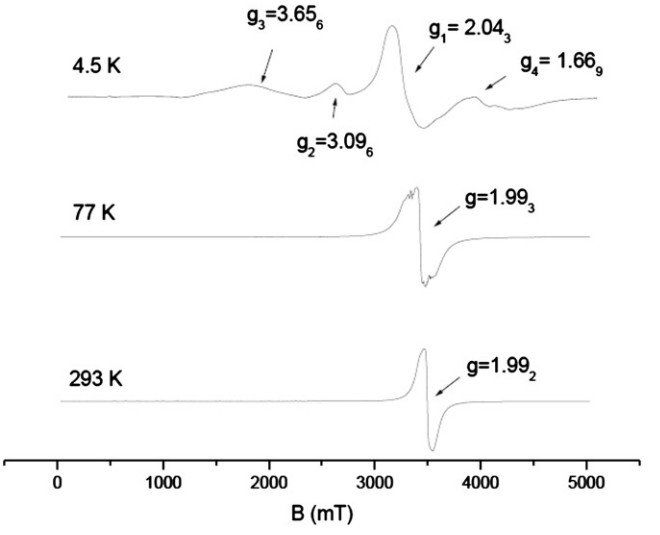

Figure 5. X-band EPR spectra of **1** at room temperature, 77 and 4.5 K.

The values for the Curie and Weiss constants, determined from the relation $1/\chi_M T = f(T)$ over the temperature range 50–300 K, are 7.65 $cm^3 mol^{-1}$ and −14.2 K. A negative value of the Weiss constant confirms the antiferromagnetic interactions between Mn centers in the crystal lattice.

The variation of the magnetization *M versus* the magnetic field *H* for **1** is shown at 2 K (figure 3b). The *M versus H* curve for **1** is linear in the whole field range and indicates magnetization of 2.65 B.M. at 5 T. The magnetic properties of **1** without water were also determined from 1.8 to 300 K in 0.5 T. The plots of magnetic susceptibility χ_M and the $\chi_M T$ product *versus T* for anhydrous **1** are given in figure 4(a). The value of $\chi_M T$ at 300 K is 5.91 $cm^3 mol^{-1} K$ (6.88 B.M.), decreasing only slightly as the temperature is lowered. Below 50 K a more evident decrease in $\chi_M T$ is observed with the continuous decrease of the temperature, reaching a value of 0.424 $cm^3 mol^{-1} K$ (1.84 B.M.) at 1.8 K. This decrease in the low temperature range is caused by the occurrence of magnetic interactions between Mn^{2+} centers. The susceptibility curve exhibits a maximum, indicating the presence of antiferromagnetic ordering with a Néel temperature (T_N) of 8.00 K.

The values for the Curie and Weiss constants, determined from the relation $1/\chi_M T = f(T)$ over the temperature range 50–300 K, are 6.18 $cm^3 mol^{-1}$ and −13.5 K. The negative value of the Weiss constant again confirms weak antiferromagnetic interactions between the Mn^{2+} centers in the crystal lattice.

The variation of the magnetization *M versus* the magnetic field *H* for **1** is shown at 2 K in figure 4(b). The *M versus H* curve is linear in whole field range with a magnetization of 2.15 B.M. at 5 T. Thus magnetic studies of **1**, with and without water, show variation in magnetic susceptibility. Although water cluster plays an important role in magnetic susceptibility, it is not clear why the susceptibility decreases without water clusters.

Table 2. EPR data for **1**.

Compound	g in 4.5 K	g in 77 K	g in 298 K
1	2.042	1.993	1.992

EPR spectra of **1** at room temperature, 77 and 4.5 K are shown in figure 5 and the values of g factor are given in table 2. The X-band solid state EPR spectrum shows noticeable variations at different temperatures. At room temperature the spectrum exhibits an isotropic signal without revealing any hyperfine structure indicative of the coordination geometry. The g_{av} is 1.99 with a peak to peak line width of 355 Gauss. At 77 K and at room temperature the g_{av} is the same except that the hyperfine splitting begins at 77 K. The manganese(II) has $I = 5/2$ and we should expect an eight line spectrum in magnetically dilute manganese(II) complex due to the hyperfine splitting. In fact, at 4.2 K we get only a four line spectrum resulting from two equivalent nuclei with $I = 5/2$.

4. Conclusions

We have reported magnetic susceptibility, with and without water clusters, and assumed that the occurrence of antiferromagnetic interactions is due to hydrogen-bonded water groups, which provide important exchange pathways for magnetic interactions between two metal centers probably by spin polarization. We also report the variable temperature EPR studies. The clusters act as an extra-framework layer between the 2-D honeycomb Mn–oxalate sheets to yield a supramolecularly assembled 3-D network.

Acknowledgments

One of the authors (K.A.S.) thanks MNNIT Allahabad for grant of a senior research fellowship. Authors are grateful to Professor P.K. Bharadwaj, Department of Chemistry, Indian Institute of Technology, Kanpur, for providing crystal data.

References

[1] M.C. Das, S.B. Maity, P.K. Bharadwaj. *Curr. Opin. Solid State Mater. Sci.*, **13**, 76 (2009).
[2] K.V. Katti, P.K. Bharadwaj, J.J. Vittal, R. Kannan. *Synth. React. Met-Org. Nano-Mat. Chem.*, **38**, 1 (2008).
[3] L.-P. Zhang, J.-F. Ma, J. Yang, Y.-Y. Liu, G.-H. Wei. *Cryst. Growth Des.*, **9**, 4660 (2009).
[4] J. Yang, J.-F. Ma, Y.-Y. Liu, J.-C. Ma, S.R. Batten. *Cryst. Growth Des.*, **8**, 4383 (2008).
[5] S.K. Ghosh, J. Ribas, M. Salah El Fallah, P.K. Bharadwaj. *Inorg. Chem.*, **44**, 3856 (2005).
[6] G. Jiang, J. Bai, H. Xing, Y. Li, X. You. *Cryst. Growth Des.*, **6**, 1264 (2006).
[7] T.K. Prasad, M.V. Rajasekharan. *Cryst. Growth Des.*, **6**, 488 (2006).

[8] B. Qing, H.L. Sun, S. Gao. *Angew. Chem. Int. Ed.*, **43**, 1374 (2004).
[9] P.R. Cuamatzi, G.V. Diaz, H. Hopfli. *Angew. Chem. Int. Ed.*, **43**, 3041 (2004).
[10] R. Custelcean, C. Afloroaei, M. Vlassa, M. Polverejan. *Angew. Chem. Int. Ed.*, **39**, 3094 (2000).
[11] S. Pal, N.B. Sankaran, A. Samanta. *Angew. Chem. Int. Ed.*, **42**, 1741 (2003).
[12] A. Mukherjee, M.K. Saha, M. Netaji, A.R. Chakravarty. *Chem. Commun.*, 716 (2004).
[13] K.V. Langenberg, S.R. Batten, K.J. Berry, D.C.R. Huckless, B. Moubaraki, K.S. Murray. *Inorg. Chem.*, **36**, 5006 (1997).
[14] S. Monikumari, V. Shivaiah, S.K. Das. *Inorg. Chem.*, **41**, 6953 (2002).
[15] J.L. Atwood, L.J. Barbour, T.J. Ness, C.L. Raston, P.L. Raston. *J. Am. Chem. Soc.*, **123**, 7192 (2001).
[16] S.K. Ghosh, P.K. Bharadwaj. *Inorg. Chem.*, **43**, 5180 (2004).
[17] J. Qu, W. Gu, L.Z. Zhang, X. Liu, D.Z. Liao. *Inorg. Chem. Commun.*, **10**, 971 (2007).
[18] K.A. Siddiqui, G.K. Mehrotra, J. Mrozinski, R.J. Butcher. *Eur. J. Inorg. Chem.*, 4166 (2008), and references therein.
[19] S.W. Benson, E.D. Siebert. *J. Am. Chem. Soc.*, **114**, 4269 (1992).
[20] R. Ludwig. *Angew. Chem. Int. Ed.*, **41**, 1808 (2001).
[21] S. Supriya, S. Manikumari, P. Raghavaiah, S.K. Das. *New J. Chem.*, **27**, 218 (2003).
[22] L.-S. Lang, Y.-R. Wu, R.-B. Huang, L.-S. Zheng. *Inorg. Chem.*, **43**, 3798 (2004).
[23] M. Zuhayra, W.U. Kampen, E. Henze, Z. Soti, L. Zsolnai, G. Huttner, F. Oberdorfer. *J. Am. Chem. Soc.*, **128**, 424 (2006).
[24] M.T. Ng, T.C. Deivaraj, W.T. Klooster, G.J. McIntyre, J.J. Vittal. *Chem. Eur. J.*, **10**, 5853 (2004).
[25] J. Xu, E. Radkov, M. Ziegler, K.N. Raymond. *Inorg. Chem.*, **39**, 4156 (2000).
[26] S.K. Ghosh, J. Ribas, P.K. Bharadwaj. *Cryst. Eng. Comm.*, **6**, 250 (2004).
[27] S. Neogi, P.K. Bharadwaj. *Polyhedron*, **25**, 1491 (2006).
[28] G.A. Jeffrey. *An Introduction to Hydrogen Bonding*, Oxford University Press, New York (1997).
[29] N.S. Ovanesyan, V.D. Makhaev, S.M. Aldoshin, P. Gredin, K. Boubekeur, C. Train, M. Gruselle. *Dalton Trans.*, 3101 (2005).
[30] *Bruker SMART, SAINT, and XPREP, AREA Detector Control and Data Integration and Reduction Software*, Bruker Analytical X-ray Instruments Inc., Madison, WI, USA (1995).
[31] G.M. Sheldrick. *SADABS, Program for Empirical Adsorption Correction of Area Detector Data*, University of Göttingen, Germany (1997).
[32] G.M. Sheldrick. *Acta Crystallogr., Sect. A*, **46**, , 467 (1990).
[33] G.M. Sheldrick. *SHELXL-97, Programme for the Refinement of Crystal Structure*, University of Göttingen, Germany (1997).